

Energy Transfer Studies of Binary Block Copolymer Blends. 1. Effect of Composition on the Interface Area per Chain and the Lamellar Size

Olga Tcherkasskaya, Shaoru Ni, and Mitchell A. Winnik*

Department of Chemistry and Erindale College, University of Toronto, 80 St. George Street, Toronto, Ontario, Canada M5S 1A1

Received August 27, 1996; Revised Manuscript Received December 17, 1996[®]

ABSTRACT: Binary blends of polyisoprene–poly(methyl methacrylate) PI–PMMA diblock copolymers with a common PMMA length and different lengths of polyisoprene blocks were prepared from samples containing a single fluorescent dye, either phenanthrene (donor) or anthracene (acceptor), at the junction point. The two pure block copolymers and their mixtures were studied by the direct energy transfer (DET) technique. All experiments point to intimate mixing of the samples over the entire composition range. These DET experiments yield the interphase volume per junction v_j and/or the ratio R/δ of the microdomain size R to the interphase thickness δ , as a function of the composition of the block copolymer mixture. Since, for these strongly segregated chains, the interface thickness is invariant with chain length and should also be constant for this set of mixtures, we can calculate from v_j and R/δ the interface area per chain and the period spacing R . Here we find that addition of up to 25 mol % of the second polymer has no effect on the lamellar longitudinal period spacing determined by the length of the major component. Changes in the structure of the binary blend occur only between these compositions.

Introduction

The twofold nature of block copolymers is manifested in self-assembly phenomena, either in bulk or in solution in the presence of a selective solvent. The inherent incompatibility between long-chain polymers induces microphase separation between the blocks, thereby forming an interface between the different components. Microdomains are characterized by interfacial properties: the surface density (number of chains per unit interfacial area) and the geometry and magnitude of the interface curvature. Segregation of single-component diblock copolymer systems has been widely investigated.^{1–7} It has been well established that the interface area occupied by a single chain increases with the chain length, while the interfacial curvature increases with the ratio of the chain lengths of the individual blocks.^{6,7} Manipulation of domain properties is, therefore, possible through adjustment of the overall molecular weight or asymmetry of the block copolymer chains. However, this method of control requires synthesis of various copolymer chains, which can be a complicated and expensive process. Blending block copolymers could provide a way of tailoring microdomain properties through simple composition variation. New structures may be obtained by changing the system composition rather than through synthesis of new copolymers.

The properties of block copolymer blends have been investigated from a theoretical point of view primarily in terms of self-consistent mean field theory and the “polymer brush” as a basic model.^{8–12} In many ways, the chains emanating from the interface of strongly segregated lamellar-forming block copolymers resemble a polymer brush. In the brush model, one examines the mixing of two chains of different lengths within a monolayer end-attached to a flat substrate. The properties of a mixed monolayer cannot be determined from simple mixing rules.⁸ Within the brush, interactions between chains of different lengths have been predicted to be attractive and to lead to homogeneous mixing.^{8,9}

The driving force for mixing is the large release in stretching free energy which increases the configurational entropy of the brush.

One of the most important factors affecting the free energy and the interfacial area per chain of the equilibrium mixed monolayer in a brush is the difference in lengths of the two-component chains. In quantitative terms, Milner, Witten, and Cates⁸ found that the relative change in free energy associated with replacing a fraction of short chains in a unimodal brush by longer ones is negligible when the volume fraction of “guests” is less than 0.2. This was explained in terms of the negligible gain in free energy when the few isolated and unstretched long chains are able to place their extra monomers in a region of small density at the edge of the brush. On the other hand, introduction of only a small amount of a shorter component into a long-chain brush leads to an immediate decrease in stretching free energy as the shorter chains increase the separation of attachment points of the longer chains. This, in turn, leads to a decrease in their stretching and steric interaction with one another.^{8–10}

Here, we should note that a theoretical analysis of equilibrium properties of a mixed monolayer in a polymer brush does not provide a full description of block copolymer microdomains. The brush model does not normally consider curvature effects. It neglects the finite interface thickness between the two blocks as well as interpenetration effects for chains emanating from opposing interfaces. As a consequence, it cannot predict phase separation except within the plane of the brush or changes in morphology.

For binary mixtures of diblock copolymers, a mean field analytical theory in the strong segregation limit has been developed by Birshtein and Zhulina⁹ and applied to lamellar and cylindrical mesophases. This analysis employs the narrow interface approximation and ignores the blending effect on the surface density. The interface area per chain is considered as an independent parameter in the minimization of the free energy density, which increases monotonically with the

[®] Abstract published in *Advance ACS Abstracts*, March 1, 1997.

increase in mean chain length. In self-assembled block copolymer systems, the surface density and interface curvature are determined by the thermodynamic equilibrium and not fixed *a priori* as in the grafted brush. In a more complete theory, both features should be allowed to vary so that they are determined by minimization of the self-assembled interface energy.

The effect of mixing on the surface density and interface curvature was treated by Dan and Safran.¹⁰ They found that, for blends of block copolymers with the same chain length but different asymmetries, the effect of mixing on the interface surface density is nonmonotonic. On the other hand, for systems with the same asymmetry but different chain lengths, the interface curvature (which is inversely proportional to the microdomain spacing) is found to have a more complex dependence on the mixture composition. It is unaffected by addition of a small fraction of either long chains or short chains, but undergoes rapid changes in the intermediate range of compositions.

A general mechanism of self-assembly of block copolymer blends has been proposed by Shi and Noolandi¹² in terms of energy balance arguments in the context of mean field theory. The formation of equilibrium ordered phases is shown to occur through a delicate balance between packing and interfacial free energies. Structural features such as surface density and interface curvature in these blends are determined by the relative changes in the stretching free energy needed to maintain constant packing density, as well as by the reduction in the interfacial tension that accompanies localization of the short blocks at the domain boundary interface.

There have been relatively few reports of experiments on binary block copolymer blends.^{13–16} The first experiments, by Hadzioannou and Skoulios^{13a} more than a decade ago, were analyzed in greater depth by Hashimoto.^{13b} Together these papers provided the experimental basis for the theoretical investigations described above. The major techniques employed have been transmission electron microscopy (TEM) and small-angle X-ray scattering (SAXS). The key questions concern the intimacy of mixing versus polymer segregation, and microscopic versus macroscopic phase separation once the limits of miscibility are exceeded.

Hashimoto and co-workers^{14b} have shown for example that for binary mixtures of lamellar forming poly(styrene-*b*-isoprene) (PS-PI) samples, in the range $\Phi_{PS} = 0.32$ – 0.66 (f_{PS} in the range of 0.35 – 0.69), the two polymers are miscible at the molecular level for all compositions if their molecular weight ratio is smaller than ~ 5 . Here Φ_{PS} is the volume fraction of PS in each block copolymer, and f_{PS} is the mole fraction of PS defined as $N_{PS}/(N_{PS} + N_{PI})$, where N_i is the degree of polymerization of the i th block. They found that when the molecular weight ratio is greater than 10, macroscopic phase separation occurs. Perhaps one of the most surprising results of these experiments is the observation that some compositions of a mixture of two lamellar-forming block copolymers exhibit a bicontinuous morphology.^{14b} This behavior was attributed to an interplay of the opposite intrinsic curvatures of the two components. Nevertheless, another blend, where the component of PS/PI volume ratio of 66/34 was mixed with a 44/56 sample, lamellar morphologies were found for all mixtures.

We are interested in the possibility of using direct nonradiative energy transfer (DET) measurements to

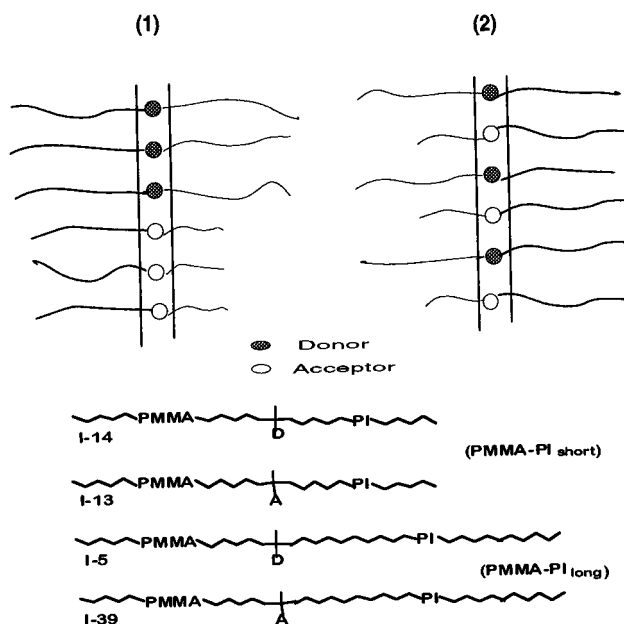


Figure 1. Above: Schematic structure of a mixed diblock copolymer monolayer with lateral phase separation (1) and with a homogeneous distribution (2) of chains of dissimilar length. Below: The four polymer samples, two with short PI chains and two with long PI chains. Each polymer is labeled at the junction with a single fluorescent dye, with D (donor) or with A (acceptor) for an energy transfer experiment.

characterize block copolymer blends. To simplify the problem, we look at a blend of two sets of poly(isoprene-*b*-methyl methacrylate) (PI-PMMA) polymers with a common PMMA block length. This is a strongly segregated system.¹⁷ With compositions of $f_{PI} = 0.58$ and 0.40 ($\Phi_{PI} = 0.56$ and 0.37), we anticipated that they would represent nearly opposing limits of lamellar-forming compositions.³¹ Because the samples have nearly identical PMMA block lengths ($N_{PMMA} \approx 220$), mixtures that maintain their lamellar morphology should represent as much as is possible the experimental analogue to the brush model.

To carry out DET experiments, one needs block copolymers labeled with fluorescent dyes, one able to act as the energy donor and the other as the acceptor. In our previous experiments on PI-PMMA block copolymers,^{17–20} we prepared pairs of samples matched in chain length and composition, one labeled at the junction with phenanthrene (the donor), and one labeled at the junction with anthracene (the acceptor). Mixtures of these two samples allow the acceptor-to-donor ratio to be varied but conserve sample morphology.

Here the polymer pairs to be mixed involve a short PI component labeled with one of the dyes and a long PI component labeled with its DET partner. Because of the way in which the dyes are attached to the polymers, they become localized in the interphase. The efficiency of DET from the donor to the acceptor directly characterizes the distribution of PI-PMMA junctions.

We conceptualize the problem in Figure 1. In the lower part of Figure 1 we show four polymers with essentially identical PMMA lengths. The samples I-5 and I-39 have "long" PI chains. The sample I-5 is labeled at the junction with a donor dye (D = phenanthrene), and I-39 is labeled at the junction with an acceptor dye (A = anthracene). Because of the similarities in the composition and chain length of these two polymers, preparing mixtures of these two samples (PMMA-PI_{long}) allows one to vary the donor-to-acceptor

Table 1. Sample Characteristics for PI-Phe(An)-PMMA Lamellar Diblock Copolymers Labeled at the Junction

sample	dye	M_n PI/PMMA	M_{total}	M_w/M_n	N PI/PMMA	N_{total}	Φ_{PI}^a	f_{PI}	f_{dye}^b	χ^c
I-5	Phe	19K/20K	39K	1.11	279/198	477	0.56	0.58	100	37
I-39	An	22K/23K	45K	1.08	323/230	552	0.56	0.59	86	43
I-13	An	10K/22K	32K	1.07	147/220	367	0.37	0.40	100	28
I-14	Phe	10K/22K	32K	1.06	147/220	367	0.37	0.40	100	28
I0-19		10K/20K	30K	1.13	147/200	347	0.39	0.42	0	27

^a Φ_{PI} and f_{PI} are the volume and mole fraction of PI block. ^b The efficiency of dye attachment (percent of labeled chains) was determined by UV analysis. ^c The Flory-Huggins interaction parameter χ was determined from DET data with a value at 25 °C of (0.077 ± 0.004) .¹⁷

ratio while maintaining the sample morphology and the period spacing. The samples I-13 and I-14 have "short" PI chains. Their mixtures maintain the morphology and period spacing of the PMMA-PI_{short} sample. To examine binary block copolymer blends with different PI chain lengths, we prepare the mixtures (I-5 + I-13) and (I-39 + I-14). A technical requirement of our experiment is that in each sample the ratio of [A/D] ≥ 1 .¹⁷⁻²⁰ Thus, two pairs of samples are needed to cover the entire composition range.

In these binary blends, one might anticipate either lateral phase separation, as shown in example 1 in Figure 1, or intimate mixing, as shown in example 2. Energy transfer is a technique that operates over a very limited length scale: Phenanthrene and anthracene undergo DET by the dipole-coupling mechanism with a characteristic Förster distance R_0 of 2.3 nm.^{17,18} According to our previous results for neat block copolymer systems,¹⁹ this value is comparable with the average distance between PI-PMMA junctions for the range of PI-PMMA molecular weights covered in the present experiments. The maximum DET distance for phenanthrene and anthracene is ~ 3.5 nm.^{17,20} Thus, the observation of energy transfer in a binary blend provides unambiguous evidence for mixing at the molecular level. Furthermore, even partial phase segregation would lead to an enhanced population of D-labeled polymers unable to transfer energy to a nearby A-labeled polymer. We would observe their contribution to the donor fluorescence decay profile. From the absence of any such contribution, we will conclude that mixing of the two polymers is intimate on the molecular scale.

Experimental Section

Synthesis and Sample Preparation. The PI-PMMA diblock copolymers were synthesized by anionic polymerization using established procedures previously described in detail.^{17,18} Here, we repeat the most important information about the polymer characterization. The number-average molecular weight M_n and polydispersity M_w/M_n of the PI blocks were analyzed by gel permeation chromatography (GPC) and were calculated from the retention times by comparison with polystyrene standards using the universal calibration curve approach. Compositions of the block copolymers and PI tacticity were determined by ¹H NMR at 400 MHz. The microstructure of the PI block was found to be 40% 1,2-addition, 55% 3,4-addition, and 5% 1,4-addition, which is typical of PI prepared by anionic polymerization in THF. These data were used to calculate M_n (GPC) for the block copolymers. Very similar values were obtained by GPC analysis of the block copolymers themselves in THF using polystyrene standards, and these traces were used to estimate M_w/M_n values. All of the diblock copolymers had a relatively narrow polydispersity ($M_w/M_n \approx 1.1$). M_n values of the PI block and of the final block copolymer were also determined by UV absorption spectroscopy by assuming 100% chromophore incorporation. From the similarities of M_n (UV) and M_n (GPC) values, the efficiency of dye incorporation f_{dye} was calculated to be close to 100%.

The volume fraction of each block was calculated by assuming that the densities of the PI and PMMA blocks are the same as those for the pure homopolymers ($\rho_{PI} = 0.913$ g/cm³ and $\rho_{PMMA} = 1.188$ g/cm³). The overall volume of block copolymer chain was calculated as the sum of PI and PMMA chain volumes. To distinguish the long and short block copolymer chains in the mixture, we label them separately with donor (phenanthrene) and acceptor (anthracene) groups, respectively. The labeling procedure has been described previously.^{17,18} The characteristics of the PI-PMMA samples examined here are presented in Table 1. All samples contain 1 wt % 2,6-di-*tert*-butyl-4-methylphenol as an antioxidant. The antioxidant does not disturb the fluorescence measurement²⁰ and is carried through all steps of sample preparation. The diblock copolymer blends were prepared from samples listed in Table 1. In these samples, the degree of polymerization of the PMMA block (N_{PMMA}) ranges from 200 to 230.

The samples for fluorescence measurements were prepared as thin films (3–6 μ m thick) in the following way: Weighed amounts of the two individual block copolymer samples were each dissolved in toluene to give solutions with a final concentration of 3.0 wt %. Carefully measured aliquots of these two solutions were mixed, and then a small amount of the mixture (~ 0.2 mL) was placed on a small quartz plate (10 \times 2.5 mm). After most of the solvent had evaporated (~ 3 h), another aliquot was added. This process was repeated three times, and then remaining traces of solvent were allowed to evaporate over 24 h at room temperature. Finally, the samples were gently annealed in a vacuum oven at 50 °C for 12 h. Some samples were heated in vacuum oven at 80 °C for 48 h before their fluorescence decays were remeasured. No changes in the decay profiles were observed.³²

Fluorescence Experiments. Fluorescence decay profiles were obtained by the time-correlated single-photon-counting technique with a pulsed lamp as the excitation source. Films were excited at the phenanthrene absorption maximum (300 nm), and the fluorescence was detected at the maximum in the fluorescence spectrum of phenanthrene (366 nm). Data were collected at 90° to the excitation, at room temperature 22 °C, to 20 000 counts in the maximum channel. The reference profile, used for the convolution analysis, was obtained by exciting a solution of *p*-terphenyl in aerated cyclohexane ($\tau = 0.96$ ns). The convolution function was compared with the experimental decay by a nonlinear least-squares optimization using the DFCM algorithm²⁴ for single-exponential decays and the Mimic algorithm²⁵ for DET decays. The minimization was of the reduced chi-squared (χ^2) function.

Data Fitting and Error Analysis. The most important feature of the DET data analysis is the examination of the shape of fluorescence decay of the isolated donor. The donor decay must be exponential in order for the lifetime of the donor τ_D to be well defined. We found that the fluorescence decays of phenanthrene attached to the junction of PI-PMMA in the neat and bimodal samples are strictly exponential in films prepared from donor-labeled polymer. To obtain the τ_D values for bimodal mixtures, we used unlabeled PI-PMMA sample (I0-19), which was added to the donor-labeled copolymer (I-5) instead of the acceptor labeled partner (I-13). The scatter in the τ_D values obtained for the pure block copolymer films, and for the block copolymer mixtures containing only donor, is less than 1% of the absolute value $\tau_D = 44.5$ ns. This value

of τ_D was introduced as a known parameter in fitting the DET decays.

The procedures of the DET data and error analysis are identical to that recently published.²⁰ The reconvolution technique used for curve fitting involves linearization of the fitting function and least-squares fitting. This technique employs More's implementation of the Levenberg–Marquardt nonlinear least-squares algorithm.²⁶ It permits one to carry out the error analyses based on the common method of approximating the residuals by an affine model.^{26,27} To estimate the reliability of the fit of the individual decays, several statistical functions are calculated. These functions include the reduced χ^2 , the weighted residuals, the shape and amplitude of the autocorrelation function of the weighted residuals, and the 95% confidence intervals for the fitting parameters of each individual decay. The values of χ^2 of the fit chosen for analysis were less than 1.5. The procedure of error estimation was based on the square root of the diagonal element (b_{jj}) of the variance–covariance matrix at the χ^2 minimum.²⁰ In this case, the standard error can be calculated as $\pm(b_{jj}^{1/2})$. This also yields the 95% confidence interval $\pm(2(b_{jj}^{1/2}))$. According to our estimates, the uncertainty of the fitting parameters for each individual donor decay was less than 3%.

Results and Discussion

We use DET experiments to study the effects of mixture composition on binary blends of PI–PMMA block copolymers. We attempt to ascertain the intimacy of mixing and the consequences of mixing on the period spacing in the system. Some aspects of this problem are ideally suited for DET experiments. For example, if one polymer is labeled with a donor dye, and the other polymer is labeled with an acceptor dye, macrophase segregation will lead to a large fraction of donors unable to undergo DET. Decay curves from such samples will contain a large contribution of the independent fluorescence of the donor. Thus, good fits of fluorescence decay data to eq 1 (see below) with a common small value of A_2 term characterizing the independent donor fluorescence can be taken as definitive evidence for intimate mixing of the junction points of the two block copolymers in the interface.

For these experiments, we choose samples of PI–PMMA with a common PMMA block length ($N_{\text{PMMA}} \approx 220$) and different PI block lengths ($N_{\text{PI}} \approx 147, 280, 320$). The common PMMA length means that changes in the period spacing will be determined by changes in the PI chain length. In this way we hope this choice of samples facilitates comparison with theoretical calculations that treat the mixing of two chains of different length within a brush.

Theoretical Considerations for DET Experiments. A common strategy for analyzing fluorescence decay profiles for energy transfer in a spatially restricted medium (in this case, the block copolymer interface) is to fit the donor decay $I_D(t)$ to the Klafter–Blumen eq:^{17, 20–23}

$$I_D(t) = A_1 \exp\left\{-\left(\frac{t}{\tau_D}\right) - P\left(\frac{t}{\tau_D}\right)^\beta\right\} + A_2 \exp\left(-\frac{t}{\tau_D}\right) \quad (1)$$

Here, the A_1 term represents the contribution of DET to the donor decay, and the A_2 term represents the independent fluorescence of the donor not involved in energy transfer. At equilibrium for strongly segregated block copolymer systems, we have shown^{17–19} that the contribution of the A_2 term in eq 1 to the total decay is less than 3–5%. This value reflects the amount of block copolymer junctions located outside of the interface, at

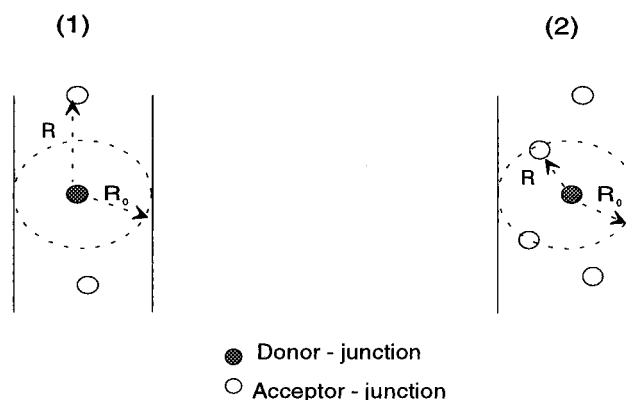


Figure 2. Schematic representation indicating the relationship between the local density of the junctions and the number of acceptor molecules per sphere within the critical Förster radius. Here the R is the average distance between junctions, and R_0 is the Förster radius.

distances too large for DET to occur. The lifetime τ_D of the donor in the absence of the acceptor is obtained from independent experiments with samples labeled only with donor chromophores. The term β is a concentration-independent parameter sensitive to the details of the local geometry of the donor–acceptor distribution.^{19,20} Because the first term in eq 1 was originally derived to describe DET on fractal lattices, where 6β is equal to the fractal (Hausdorff) dimension, in restricted geometries, 6β is often referred to as the “apparent dimension” of the system.^{21–23}

According to the theory of DET in a restricted geometry, the parameter P depends upon the local density of acceptors within a certain distance of an excited donor:^{21–23}

$$P = c_A g^\beta \Gamma(1 - \beta) \quad (2)$$

Here c_A is the number of acceptor molecules that occupy a “quenching sphere”, centered on a donor, with a radius equal to the critical Förster distance R_0 for energy transfer. The term $\Gamma(1 - \beta)$ is the complete gamma function, and g is the orientation factor, which for random orientation of immobile dyes has a value of 0.711.¹⁸ For block copolymer interfaces, the number of acceptors per sphere of radius R_0 is inversely proportional to the interface volume v_j occupied by a single chain. We note that, in these experiments, both dyes are attached to the copolymer junctions. As a consequence, the larger the interface volume v_j per junction, the lower the number of acceptors per quenching sphere. This relationship is illustrated in Figure 2.

The number of acceptors c_A per quenching sphere can be related to the interface volume v_j through the expression

$$P = \left(\frac{4}{3}\pi R_0^3\right) \frac{q_{ac}}{v_j} g^\beta \Gamma(1 - \beta) \quad (3)$$

where q_{ac} is the number fraction of the chains labeled with the acceptor and the ratio (q_{ac}/v_j) is the local concentration of acceptors in the interphase volume. We introduce the parameter P' as

$$P' = \frac{P}{g^\beta \Gamma(1 - \beta)} = \left(\frac{4}{3}\pi R_0^3\right) \frac{q_{ac}}{v_j} \quad (4)$$

to obtain a simple relationship between the fitting parameter P and the fraction of chains labeled with acceptor in the system of interest. Equation 4 allows us to determine v_j values directly from the fluorescence decay profiles. This analysis makes no assumptions about the composition of the system or its global morphology and thus should apply equally well to intimately mixed copolymer blends. The only assumption in this model with respect to blends is the random distribution of junctions in the interphase. The other parameters (P , q_{ac} , R_0) needed for the evaluation of v_j can be obtained from independent experiments.

Another way of analyzing the DET data is based upon the relationship between the local dye concentration and the volume fraction of interphase in the system of interest. We have shown recently¹⁸ that the DET efficiency depends upon the global acceptor concentration $C_{A,0}$ in the block copolymer films as

$$P = \frac{4\pi R_0^3 N_{Av}}{3\lambda\Phi_B} C_{A,0} \quad (5)$$

Here N_{Av} is Avogadro's number, and Φ_B is the volume fraction of the minor B phase. The volume fraction of interphase is expressed through the product $\lambda\Phi_B$, where the parameter λ is the volume ratio of the interphase to that of minor phase. For lamellar microdomains, a geometric analysis of the system yields¹⁸

$$\lambda = \delta/R_B \quad (6)$$

where δ is the interface thickness and R_B is the half-length of the lamella of the minor B component.³⁰ Thus, if one knows the value of the global acceptor concentration $C_{A,0}$ and volume fraction of the minor component Φ_B for a bimodal copolymer mixture, then one can obtain through eqs 5 and 6 the volume of interphase and the size of the lamellar phase composed of the minor component.

Numerical Estimates of the Model Parameters. To estimate the microdomain size for binary block copolymer blends by means of eqs 5 and 6, we need to calculate the global acceptor concentrations in the films prepared from mixtures of labeled block copolymers with different chain lengths. Since the block copolymers are labeled only at the junction, and each polymer molecule contains one dye, the global dye concentration in the neat sample is equal to the reciprocal molar volume ($V_{PI-PMMA}$) of the block copolymer.

$$C_{dye} = 1/V_{PI-PMMA} \quad (7a)$$

We calculate the molar volume as the sum of the individual block volumes:

$$V_{PI-PMMA} = V_{PI} + V_{PMMA} = \frac{M_{PI}}{\rho_{PI}} + \frac{M_{PMMA}}{\rho_{PMMA}} \quad (7b)$$

where M_i is the molar mass of the individual block and ρ_i is its density.

For bimodal mixtures, the dye concentration $\langle C_{dye} \rangle$ can be calculated through the mean molar volume, which we obtain as a linear average of the molar volumes V_j of the components.

$$\langle C_{dye} \rangle = \frac{1}{q_{short} V_{PI-PMMA}^{short} + q_{long} V_{PI-PMMA}^{long}} \quad (8)$$

In eq 8 the q_i is the mole fraction of the block copolymer with the short ($i = s$, short) or long ($i = l$, long) component. The global acceptor concentration $\langle C_{A,0} \rangle$ in the bimodal mixture is proportional to the mole (number) fraction of the acceptor labeled chains:

$$\langle C_{A,0} \rangle = q_{ac} \langle C_{dye} \rangle \quad (9)$$

In the same way, we calculate the overall volume fraction of the minor (PI) component³⁰ $\langle \Phi_B \rangle$ in the copolymer mixture:

$$\langle \Phi_{PI} \rangle = \frac{q_{short} V_{PI}^{short} + q_{long} V_{PI}^{long}}{q_{short} V_{PI-PMMA}^{short} + q_{long} V_{PI-PMMA}^{long}} \quad (10)$$

To interpret the P values obtained from DET experiments in terms of the composition of the system, we need four parameters. We calculate three of these parameters ($\langle C_{dye} \rangle$, $\langle C_{A,0} \rangle$, $\langle \Phi_{PI} \rangle$) from eqs 7–10. The fourth parameter is the orientation factor g (c.f. eq 2), for which we use the value 0.771. This value is appropriate to a random ensemble of immobile dyes. If, however, there is a strong mutual orientation of dyes in the interface, this number may be in error. The magnitude of any error here is likely to be small because the orientation factor enters into P as g^β . Since the parameter β is a rather small number ($\beta \approx 0.25$), g^β has a value close to unity.²¹

The experiment proceeds as follows: A series of PI–PMMA blends were prepared using the samples described in Table 1. In these samples, the degree of polymerization of the PMMA block (N_{PMMA}) ranged from 200 to 230, which we treat as being very similar. The samples with the shorter PI block had $N_{PI} = 147$, whereas those with the longer PI block had $N_{PI} = 279$ or 323. The different blend samples contained different amounts of sample with the longer PI block. DET measurements were carried out, and from the fit of the fluorescence decay curves to eq 1, the values of the (A_2 , P , β) parameters were extracted. Then, the values of v_j , $\lambda\Phi_B$, λ , and, finally, R/δ , were calculated by means of eqs 2–10. These parameters are then considered as a function of the block copolymer mixture composition.

The Structure of Binary Blends. We begin our experiments by examining DET kinetics in pairs of donor- and acceptor-labeled polymers of approximately the same chain length and composition. These data are shown in Figure 3 as a plot of P versus global acceptor concentration $C_{A,0}$. The filled circles on line 1 are from mixtures of samples I-5(Phe) + I-39(An), polymers with the longer PI chains (PMMA–PI_{long}). The filled triangles on line 2 are from mixtures of samples I-14(Phe) + I-13(An) (i.e., PMMA–PI_{short}), which represent the polymers with the shorter PI chains. As in our previous experiments,¹⁷ the P values are proportional to $C_{A,0}$, and the line through the data passes through the origin. The slope of each plot is determined by the thickness of the PI lamella. For both sets of experiments, the A_2 term in the fluorescence decay represents $\sim 3\%$ of the total signal (top portion of Figure 3).

Representative fluorescence decay curves for experiments on binary blends of polymers of different PI chain lengths are shown in Figure 4. One can see the strong deviation of the donor fluorescence decay from a monoexponential shape, when the short chains labeled with acceptor (sample I-13) are introduced to the structure formed by the longer chains labeled with donor (sample I-5). The individual curves gave good fits

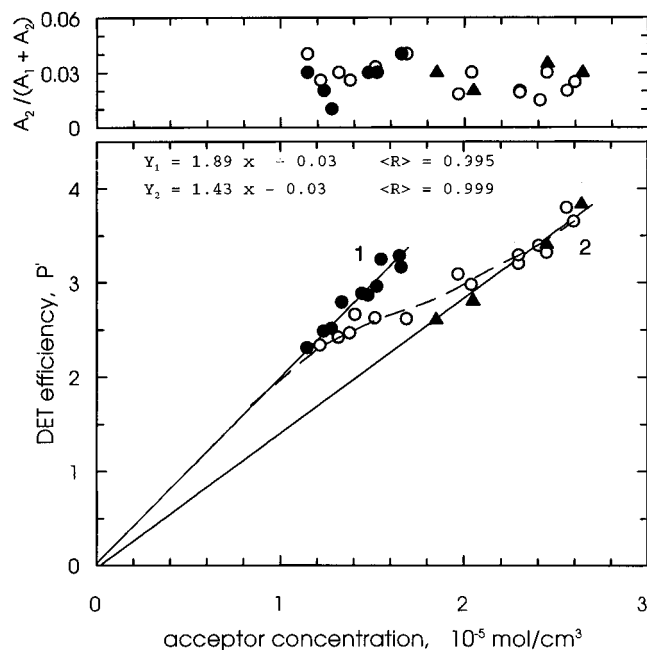


Figure 3. Variation of the fitting parameter P versus the global acceptor concentration $\langle C_{A,0} \rangle$ in PI-Phe(An)-PMMA films. The filled circles on lines 1 and 2 refer to PI-PMMA samples with similar length and composition: (●) blend of samples I-5 + I-39 (PMMA-PI_{long}; $N_{PI} = 279, 323$); (▲) blend of samples I-13 + I-14 (PMMA-PI_{short}; $N_{PI} = 147$). The open circles (○) refer to bimodal mixtures of these samples, e.g., (I-5 + I-13) and (I-39 + I-14). The top portion of the figure presents for each sample the fraction of donor-labeled chains that do not undergo energy transfer as determined by fitting each decay profile to eq 1.

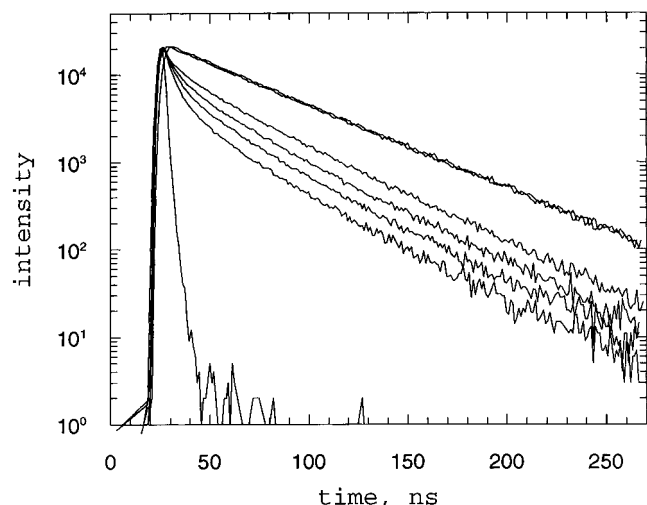


Figure 4. Fluorescence donor decays obtained for mixtures of PI-Phe(An)-PMMA samples. The curves represent blends of the samples I-5(Phe) and I-13(An) with increasing mole fraction of the acceptor-labeled shorter PI chains (from top to bottom): 0, 0.39, 0.55, 0.65, and 0.76. Upper decay represents samples containing only donor in which the PI short chains fraction has a value of 0 (I-5) and/or 0.55 (I-5 + I-09). The shapes of the weighted residuals and of the autocorrelation function of the weighted residuals for all cases have the character of random noise with an amplitude less than 3.5 and 0.3, respectively.

to eq 1. The results from these experiments with binary blends are shown as the open circles in Figure 3. These circles correspond to mixtures of I-5(Phe) with I-13(An) and I-39(An) with I-14(Phe). With these two sets of samples, we can cover a wide range of (PI_{long} - PI_{short}) mixtures with a correspondingly large range of acceptor concentrations. The first result of importance in Figure

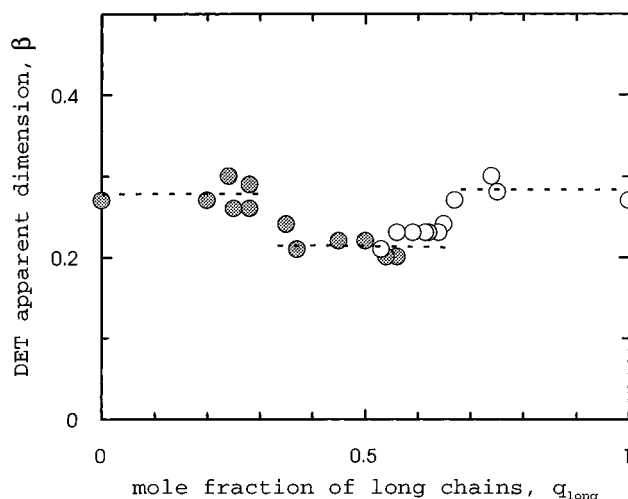


Figure 5. Dependence of the DET fitting parameter β upon the composition of the block copolymer mixture, plotted as a function of the fraction of the longer PI chains q_{long} , for the binary blends of I-5 with I-13 (filled symbols) and I-39 with I-14 (open symbols).

3 is that the A_2 term in the fluorescence decay curves from all of these mixtures falls in the same range (3% of the total signal) as that found for the samples with a common PI chain length. This establishes that mixing of the junction points of the two polymers with different chain length is intimate on the scale of DET. Two PI-PMMA block copolymers are totally miscible on the molecular level at all compositions and there is no tendency for phase separation.

We also note that the P values obtained for bimodal mixtures deviate from the linear behavior obtained for neat samples but, nevertheless, increase continuously with the global acceptor concentration $\langle C_{A,0} \rangle$. Line 1 in Figure 3 represents the data for the polymers with the longer PI chain ($N_{PI} = 279, 323$). The presence of two open circles along this line suggests that addition of a shorter chain component does not affect the period spacing. Line 2 represents the data for the polymers with the shorter PI chain ($N_{PI} = 147$). The six open circles on this line suggest that the presence of a small amount of longer PI component also does not affect the period spacing determined by the shorter polymer.

The parameter β obtained from the decay curves also contains information about the distribution of junctions in the block copolymer interfaces (see eq 1). We note that, in previous experiments, we obtained values of $\beta = 0.28$ for monodisperse samples of PI-PMMA,¹⁷ whereas for samples of PS-PMMA, we obtained values of $\beta = 0.22$.¹⁸ These β values were independent of the acceptor concentration (i.e., of the composition of the donor and the acceptor-labeled polymers) as long as the ratio of acceptor to donor $[A/D]$ was larger than unity. In Figure 5 we plot the values of the β parameter as a function of PI-PMMA blend composition. In all cases reported here, the $[A/D]$ is greater than unity. We see a different type of behavior in Figure 5. Here values of β are equal to 0.28 over the range $q_{long} = 0-0.3$ and $q_{long} = 0.7-1.0$, but exhibit a sudden transition to a value of 0.22 for the intermediate range of compositions.

Values of β are difficult to interpret unambiguously. Simulations of DET in restricted geometries with random donor-acceptor distributions suggest that β is primarily sensitive to features of the distribution at the edges of the confining space. On the other hand, for PI-PMMA interfaces, we have observed a decrease in

Table 2. Interface Volume per Junction for Monodisperse PI-PMMA Films

sample ^a	morphology	N_{PI}/N_{PMMA}	v_j , ^b nm ³	v_j , ^c nm ³
I-17, 12	lamella	132/172	10.1	10.4
I-13, 14	lamella	147/220	9.2	9.0
I-5, 39	lamella	279/198	10.9	11.0
I-36, 37	lamella	279/265	12.0	11.5
I-21, 22	sphere	147/509	9.0	9.2

^a Sample characterization was reported in ref 17. ^b The volume per junction was determined for a series of monodisperse samples through the R/δ ratio.¹⁹ ^c Volume per junction determined with eq 4 from fits to individual fluorescence decay profiles.

β , or more precisely, a crossover to a lower value, for $[A/D] < 1$,²⁰ corresponding to a mean donor-acceptor separation greater than the interface thickness. From this very limited point of view, the changes in β point to changes in the donor-acceptor distribution in the interface, in terms of the interfacial area per chain σ , the interface thickness δ , or the magnitude of fluctuations of the joints in the interface. The most important information about these binary blends comes from the influence of composition on the magnitude of the P parameter as shown in Figure 3. The remainder of this paper is devoted to examining these effects in more detail.

Interface Volume per Junction. The interphase volume v_j per junction is a sensitive parameter of the structure of mixed microdomains. In strongly segregated systems, this volume, which is the product of the interfacial area per chain σ times the interface thickness δ , provides information about σ because δ is independent of chain length¹⁹

$$v_j = \sigma\delta \quad (11)$$

Recently we reported¹⁹ a method for calculating v_j values from DET data based on the relationship between interface volume v_j per junction and the "minor phase-to-interphase" ratio R_B/δ . Here, eqs 3 and 4 provide a method to obtain values of v_j directly from the fitting parameter P for each fluorescence decay curve. This allows us to obtain v_j values for experiments on binary blends. To test the consistency of the two methods, we have reanalyzed the decay curves for the experiments described in ref 19 and compare the values of v_j obtained in Table 2. We see that similar values are obtained by both approaches, which emphasizes the usefulness of eq 4 to obtain these values.

The variation of the interface volume per junction with the composition of the bimodal mixtures is shown in Figure 6. The circles represent the experimental values, while the dashed line represents a linear averaging of the v_j values obtained for the individual PI-PMMA components. One can see that the composition dependence of v_j is strongly nonmonotonic, passing through both a maximum and a minimum between the composition limits. For addition of small amounts of "guest polymer" to a sample, changes in v_j composition behave as expected: The longer the chain in a lamellar phase, the larger the volume occupied at the interface.^{6,7} This represents a balance between the increased stretching of the longer chain and the increased surface area in the system. The surface tension tends to decrease the area per chain or, in the language of the brush model, to increase the "grafting" density, whereas mutual repulsion between adjacent chains tends to increase the area per chain. The latter effect becomes

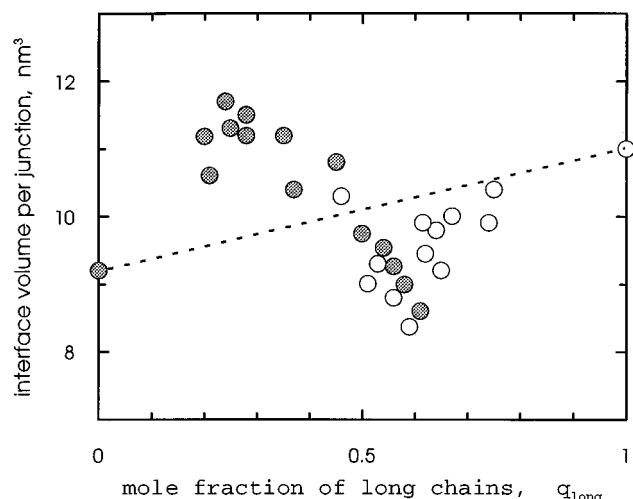


Figure 6. Variation of the interface volume v_j per junction versus the composition of the bimodal mixture, characterized by the fraction of the longer PI chains q_{long} , for the samples shown in Figure 5.

larger in magnitude with the size of the blocks in each component.^{6,7}

When a guest longer chain is added to a system, it leads to an increase in the lateral repulsion between chains confined to the microdomain composed of the shorter chains. The system responds by an increase in v_j . When a guest shorter chain is added to a system, it leads to a decrease in lateral repulsion interactions. The system undergoes a relaxation of stretching, particularly at the periphery of the short-chain brush, and v_j decreases. In both cases, the segment density in the microdomain should be identical to that of bulk polymer. To satisfy the demand for uniform volume filling of space, the long and short chains become stretched to different extents, and the extent of stretching is nonuniform along the chain contour. Thus, the observation of the increase of v_j at small values of q_{long} and the increase of v_j as q_{long} approaches unity are consistent with the expected behavior of binary blends.

The unusual result here is the decrease of the interface volume per junction with the increase in the fraction of long chains in the intermediate range of the mixture compositions. A similar result can be obtained by a somewhat different analysis of the DET data in terms of the interphase volume fraction $\lambda\Phi_{PI}$ in the system. We calculate $\lambda\Phi_{PI}$ by means of eq 5 through the value of the fitting P parameter and the average global acceptor concentration in the copolymer mixtures. For the PI-PMMA samples investigated, the PI volume fraction varies from 0.37 to 0.56. It leads to a change in $\lambda\Phi_{PI}$ from 0.19 to 0.17: The longer is the lamella, the smaller is the interphase volume fraction, although the difference between these two samples is rather small. Even at the scale of this small difference in $\lambda\Phi_{PI}$ values, the data of Figure 7 show a clear nonmonotonic variation of the interphase volume fraction with composition of the block copolymer mixture. Thus, we conclude that the volume fraction of interphase, and/or the volume per junction (which are both calculated from the parameter P), varies with the composition of the bimodal block copolymer mixture in a nonmonotonic way.

These results appear to be different than those obtained by Hadziioanou and Skoulios.^{13a} They examined a series of PS-PI di- and triblock copolymer blends by SAXS and, for each blend composition, calculated the

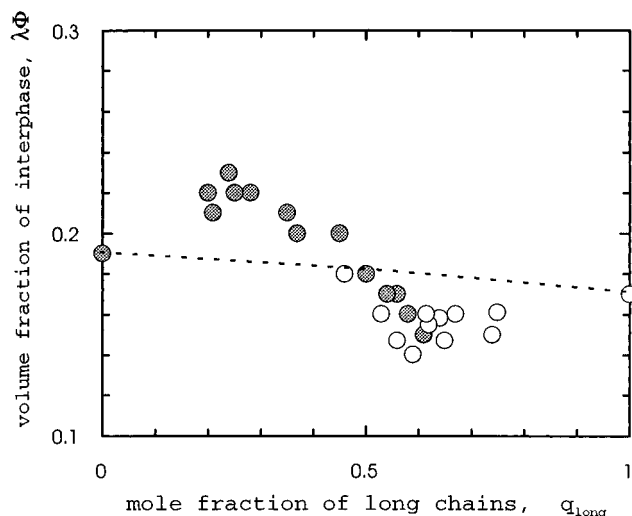


Figure 7. Variation of the interphase volume fraction $\lambda\Phi_{PI}$ versus the composition of the block copolymer mixture, characterized by the fraction of the longer PI chains q_{long} , for the samples shown in Figure 5.

mean interface surface area per chain $\langle\sigma\rangle$ from the period spacing and the mean molecular volume of the chain. In their various examples, one finds at first glance that the $\langle\sigma\rangle$ values calculated in this way lie very close to the mean values representing a linear composition average of the σ values of the two pure polymers. Hashimoto^{13b} reanalyzed the data for one particular diblock copolymer blend and deduced that $\langle\sigma\rangle$ scales as $\langle M_n \rangle^{1/3}$, where $\langle M_n \rangle$ represents the mean molecular weight of the blend. Closer inspection of Figure 2 in ref 13b indicates that, upon addition of the longer polymer (both have $f_{PS} = 0.50$), mean surface area per chain $\langle\sigma\rangle$ increases at small q_{long} and lies above the mean value line, remains flat over the intermediate range of compositions crossing to below the mean value line, and then increases once again as q_{long} attains unity. Other examples in ref 13a appear to show nonrandom deviations in plots of $\langle\sigma\rangle$ versus q_{long} from the mean value line. While we may be asking too much of the data from these early and pioneering measurements, these deviations emphasize the importance of further experiments to examine the interface structure in block copolymer blends.

Domain Size. An important question in the context of the present investigation is the effect of composition on the lamellar size. From DET experiments, we can obtain directly the ratio of the lamellar half-length R_{PI} to the interface thickness δ (see eqs 1–6). For PI-PMMA, we have found that the interface thickness δ has a value of 2.6 nm, independent of the lengths of the PMMA and PI blocks.¹⁷ In the analysis that follows, we presume that the value of δ is conserved in the binary blends we examine. We take this assumption to be a reasonable working hypothesis because, for strongly segregated systems, the interface thickness is determined primarily by local interactions. The magnitude of δ depends primarily upon the thermodynamic immiscibility of the dissimilar monomer units (the χ parameter) and the flexibility (segment length) of the two copolymer chains.^{1–5}

In Figure 8 we plot the R_{PI}/δ ratio as a function of the mixture composition. The R_{PI}/δ values were calculated by means of eqs 5 and 6, and the mean values of the parameters, required for the R_{PI}/δ calculations, were obtained through eqs 7–10. One can see that addition

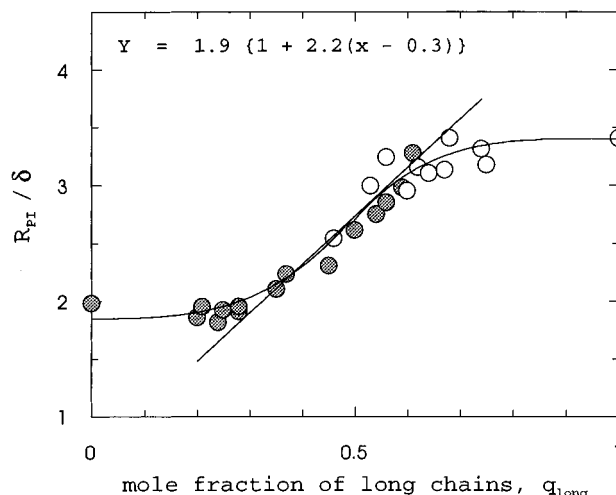


Figure 8. Variation of the R_{PI}/δ ratio ($\delta = 2.6$ nm) versus the composition of the block copolymer mixture, characterized by the fraction of the longer PI chains q_{long} , for the samples shown in Figure 5.

of significant amounts of long component as a guest to the short polymer matrix, or short component as a guest to the long polymer matrix, has almost no influence on R_{PI}/δ . Between a fraction of long chains q_{long} of ~ 0.28 – 0.63 , there is a marked and steady increase in R_{PI}/δ values, between the limiting values for the shorter and longer components. Since δ should be constant over this set of samples, R_{PI}/δ measures the change in the PI lamellar spacing. This leads to the conclusion that when the fraction of guests is less than a certain rather substantial amount, there is no change in the lamellar longitudinal spacing.

In the intermediate range of bimodal compositions, the lamellar size continuously increases as a function of q_{long} . Here the change in the length of the PI lamella can be approximately described by the linear equation

$$R_{PI}/\delta = 1.9[1 + 2.2(q_{long} - 0.3)] \quad (12)$$

In equation 12, the numerical coefficient (1.9) corresponds to the experimental R_{PI}/δ value obtained for the PI lamella with the shorter PI chain length ($N_{short} = 147$). The second coefficient (2.2) is very close in magnitude to the fractional increase in length of the PI component (we use for N_{long} the average value for PI chain lengths of samples I-5 and I-39):

$$\gamma = N_{long}/N_{short} = 301/147 = 2.1 \quad (13)$$

The coefficient (0.3) indicates the limit of the range of compositions for which this linear approximation is applicable. The data described by eq 12 can also be fitted to a power law, as predicted by Birshtein and Zhulina^{9a,b} and as reported by Hashimoto.^{13b} The major difference between our results and the theoretical prediction, is that we find ranges at both ends of the composition spectrum where there is no change in the R_{PI} . One implication of this result is that there are critical compositions where the lengths of the domains begin to change.

Critical Blend Compositions. To understand how the onset composition for the lamellar spacing changes is related to the properties of the components, we consider the mean volume per chain $\langle v_{chain} \rangle$ of the PI blocks in the PI microdomains. The chain volume can be expressed as a product of the interfacial area σ occupied by a single block copolymer times the height

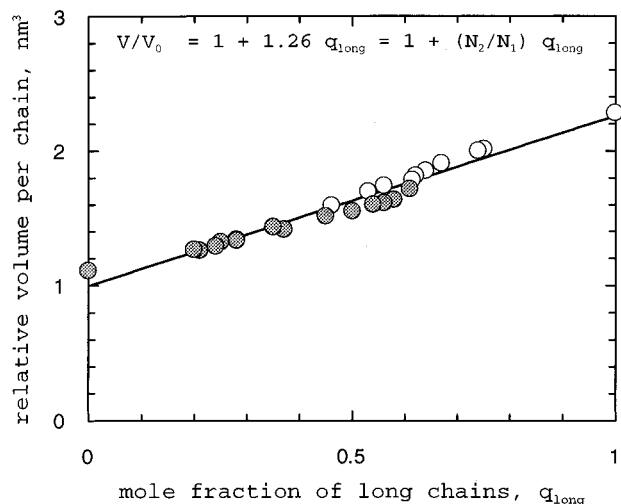


Figure 9. Variation of the mean PI chain volume ($\langle v_{\text{chain}} \rangle$) versus the composition of the block copolymer mixture, characterized by the fraction of the longer PI chains q_{long} , for the samples shown in Figure 5.

R_{PI} of the PI brush. Since $v_j = \sigma\delta$, we can calculate $\langle v_{\text{chain}} \rangle$ from the experimental data as follows:

$$\langle v_{\text{chain}} \rangle = \sigma R_{\text{PI}} = v_j (R_{\text{PI}}/\delta) \quad (14)$$

The variation of the mean PI chain volume with composition of the bimodal mixture is shown in Figure 9. One sees that, in spite of the nonmonotonic composition effect on the interface volume per junction (Figure 6) and on the lamellar spacing as expressed by R_{PI}/δ (Figure 8), the mean chain volume is simply proportional to the composition of the mixture. The slope of this plot (1.26) is very close to the ratio of the molecular weights (1.3) for the two block copolymers:

$$\langle v_{\text{chain}} \rangle = v_{\text{short}} [1 + (N_{\text{long}}/N_{\text{short}}) q_{\text{long}}] \quad (15)$$

In terms of average chain volume, eq 15 is very similar to the result of Birshtein and Zhulina^{9a,b} for a mixed flat layer. In their analysis, they assumed a fixed interface area per chain and found a linear increase in the period height with composition. From this point of view, there is agreement between experiment and theory.

We now consider the composition of the system where changes in R_{PI}/δ occur. We begin by calculating the relative change in PI chain volume compared to that of one of the components in its own microdomain:

$$\frac{\Delta v}{v} = \frac{v_{\text{chain}} - \langle v_{\text{chain}} \rangle}{v_{\text{chain}}} = 1 - \frac{\langle v_j \rangle}{v_j} \quad (16)$$

Here v_{chain} is the volume per chain of the PI in either of the pure block copolymer components, and $\langle v_{\text{chain}} \rangle$ is the mean value for the mixture. The term $\langle v_j \rangle$ refers to the experimental value of v_j for the mixtures taken from Figure 6 corresponding to the maximum and minimum values. These correspond to the values of $q_{\text{long}}^{\text{crit}}$ where the changes in R_{PI}/δ begin (Figure 8). In this way we find that adding long PI chains ($q_{\text{long}}^{\text{crit}} = 0.25$, $\langle v_j \rangle = 11.7 \text{ nm}^3$) to the short polymer matrix ($v_j = 9.3 \text{ nm}^3$) gives a value of $|\Delta v/v| = 0.25$. Similarly, adding short PI chains ($q_{\text{short}}^{\text{crit}} = 1 - q_{\text{long}}^{\text{crit}} = 0.40$, $\langle v_j \rangle = 8.2 \text{ nm}^3$) to the long polymer matrix ($v_j = 11.0 \text{ nm}^3$) also gives a value of $|\Delta v/v| = 0.25$. Thus, in our experiments, it appears that the lamellar spacing in a binary blend remains constant

(under the assumption of invariant δ) until 25% of the second component is added. Beyond that value, the stability limit of the lamella is exceeded.

Summary and Conclusions

Our results suggest that the rearrangement of block copolymer lamellae induced by the chain length heterogeneity can be considered as a two-stage process. Initially, when the amount of the second component is small, the length heterogeneity in one of the components does not effect the lamellar size but has a pronounced effect on the area per chain σ at the interface. From a brush model perspective, long chains introduced into the brush increase the repulsion between neighboring chains, which leads to an increase in σ . This effect is sufficiently strong that the increase in σ is significantly larger than the mean value calculated from the composition of the blend. When short chains are added to a brush of longer chains, again no change in the brush height is found when the amount of short chains is small. Here the area per chain at the interface decreases substantially due to a relaxation of repulsion between neighboring chains.

In stage 2, when the composition of the mixture exceeds $\sim 25 \text{ mol } \%$ of the guest, the brush height begins to change and increases in a monotonic manner until the host composition is reduced to 25 mol %. In this range of compositions, the measured values of the interface volume per junction v_j undergo pronounced changes (Figure 6), decreasing in our samples from a maximum at $q_{\text{long}} \approx 0.25$ to a minimum at $q_{\text{long}} \approx 0.6$. It is significant from the point of view of our experiments, that the maximum and minimum in v_j correspond to the compositions between which the lamellar spacing (as inferred from R/δ) evolves. It is also noteworthy that these compositions correspond to the crossover in the DET exponent β as shown in Figure 5. The reorganization of the system involves important changes at the level of the block copolymer interface.

One of the most surprising results of present experiments is the nonmonotonic variation with composition of the interface volume per chain (Figure 6). With the assumption that the interface thickness is invariant with blend composition, this behavior implies that it is the interface area per chain (see eq 11) which exhibits this behavior. This result is inconsistent with theoretical predictions in the strong segregation limit (SSL). Semenov²⁸ has shown that, in the framework of SSL theory, the interface area per chain increases with the long chain fraction. The change of area per chain is negligible for small amounts of added longer polymer. The total period and the PI period spacing smoothly increase with increasing fraction of longer chains. No plateau, for any amount of added long chains, is predicted. Addition of fluctuation corrections to the SSL theory does not change the main character of this dependence. At the same time, Semenov²⁸ has found that fluctuation corrections to mean field theory can give rise to some similarities to the DET experimental results: an initial increase and a then a decrease of the apparent area per junction with long-chain fraction. Thus, in the framework of mean field theory with fluctuation corrections, a nonmonotonic composition effect on the interface area per chain is predicted. However, a decrease of the area per chain below that of the pure short-component value (see Figure 6) is still difficult to explain.

Another insight into the events occurring in the system is possible from the theoretical analysis of a

brush of mixed chain lengths by Klushin and Skvortsov.²⁹ They considered brush dynamics, and drew an analogy between the chemical potential of a grafted brush and of a polymer in a longitudinal flow undergoing a coil-to-stretch transition. They found that the chemical potential in the grafted brush is exactly at the critical value for chain elongation. They wrote²⁹ that "each chain in the brush is in the middle of a coil-to-stretch transition, which gives at least a formal explanation for the anomalous amplitude of the end-to-end distance fluctuations", which they found in their analysis of the system. They then considered the addition of a small amount of shorter chains of length K to the brush of longer chains of length N . Since each short chain is surrounded by the longer chains, they experienced the mean field determined by the longer chains. Since shorter chains are less easily deformed, the field will appear subcritical to them. Klushin and Skvortsov then examine the coil-to-stretch transition of the shorter chains as they are allowed to grow longer (i.e., as $K \rightarrow N$). As K approaches N , fluctuations in the brush height increase dramatically, suggesting that chains in a monodisperse brush are close to a second-order phase transition.

We now speculate that the range of compositions for which R/δ evolves corresponds to a coil-stretch transition for both components. This would be accompanied by larger amplitude fluctuations not only of the chain-end separation from the interface but also of the junction distribution in the interface. These larger amplitude fluctuations might well explain the crossover in β in the energy transfer measurements.

Acknowledgment. The authors thank the donors of the Petroleum Research Fund, administered by the American Chemical Society, and NSERC Canada for their support of this research. We appreciate helpful discussions and critical comments from Drs. E. B. Zhulina, A. N. Semenov, J. Noolandi, and F. S. Bates.

References and Notes

- (1) Bates, F. S.; Fredrickson, G. H. *Annu. Rev. Phys. Chem.* **1990**, *41*, 525.
- (2) Bates, F. S. *Science* **1991**, *151*, 898.
- (3) (a) Helfand, E.; Tagami, Y. *J. Chem. Phys.* **1972**, *56*, 3592. (b) Helfand, E.; Wasserman, Z. R. *Macromolecules* **1976**, *9*, 879; **1978**, *11*, 960; **1980**, *13*, 994.
- (4) Hong, K. M.; Noolandi, J. *Macromolecules* **1981**, *14*, 727.
- (5) (a) Semenov, A. N. *Sov. Phys. JETP* **1985**, *61*, 733. (b) Semenov, A. N. *Macromolecules* **1989**, *22*, 2849; **1993**, *26*, 2273.
- (6) Zhulina, E. B.; Semenov, A. N. *Vysokomol. Soed. A* **1989**, *31*, 177.
- (7) Birshtein, T. M.; Zhulina, E. B. *Polymer* **1984**, *25*, 1453; **1989**, *30*, 170; **1990**, *31*, 1312.
- (8) Milner, S. T.; Witten, T. A.; Cates, M. E. *Macromolecules* **1988**, *22*, 853.
- (9) (a) Birshtein, T. M.; Lyatskaya, Yu. V.; Zhulina, E. B. *Polymer* **1990**, *31*, 2185; **1992**, *33*, 2750. (b) Zhulina, E. B.; Birshtein, T. M. *Polymer* **1991**, *32*, 1299. (c) Zhulina, E. B.; Lyatskaya, Yu. V.; Birshtein, T. M. *Polymer* **1992**, *33*, 332.
- (10) Dan, N.; Safran, S. A. *Macromolecules* **1994**, *27*, 5766.
- (11) Shull, K. R.; Winey, K. *Macromolecules* **1992**, *25*, 2637.
- (12) Shi, A. Ch.; Noolandi, J. *Macromolecules* **1994**, *27*, 2936; **1995**, *28*, 3103.
- (13) (a) Hadziiaouanno, G.; Skoulios, A. *Macromolecules* **1982**, *15*, 267. (b) Hashimoto, T. *Macromolecules* **1982**, *15*, 1548.
- (14) (a) Hashimoto, T.; Koizumi, S.; Hasegawa, H.; Izumitani, T.; Hyde, S. T. *Macromolecules* **1992**, *25*, 143. (b) Hashimoto, T.; Yamasaki, K.; Koizumi, S.; Hasegawa, H. *Macromolecules* **1993**, *26*, 2895. (c) Hashimoto, T.; Koizumi, S.; Hasegawa, H. *Macromolecules* **1994**, *27*, 1562. (d) Koizumi, S.; Hasegawa, H.; Hashimoto, T. *Macromolecules* **1994**, *27*, 4371.
- (15) Saito, R.; Kotsubo, H.; Ishizu, K. *Polymer* **1994**, *35*, 1580.
- (16) Baek, D. M.; Han, C. D.; Kim, J. K. *Polymer* **1992**, *33*, 4821.
- (17) Tcherkasskaya, O.; Ni, S.; Winnik, M. A. *Macromolecules* **1996**, *29*, 610.
- (18) Ni, S.; Zhang, P.; Wang, Y.; Winnik, M. A. *Macromolecules* **1994**, *27*, 5742 and references therein.
- (19) Tcherkasskaya, O.; Ni, S.; Winnik, M. A. *Macromolecules* **1996**, *29*, 4241.
- (20) Tcherkasskaya, O.; Spiro, J. G.; Ni, S.; Winnik, M. A. *J. Phys. Chem.* **1996**, *100*, 7114 and references therein.
- (21) (a) Klafter, J.; Blumen, A. *J. Phys. Chem.* **1984**, *80*, 875. (b) Klafter, J.; Blumen, A. *J. Lumin.* **1985**, *34*, 77. (c) Blumen, A.; Klafter, J.; Zumofen, G. *J. Chem. Phys.* **1986**, *84*, 1397. (d) Levitz, P.; Drake, J. M.; Klafter, J. *J. Chem. Phys.* **1988**, *89*, 5224. (e) Drake, J. M.; Klafter, J.; Levitz, P. *Science* **1991**, *251*, 1574.
- (22) Klafter, J.; Drake, J. M., Eds.; *Molecular Dynamics in Restricted Geometries*; Wiley: New York, 1989.
- (23) Kellerer, H.; Blumen, A. *Biophys. J.* **1984**, *46*, 1.
- (24) Zuker, M.; Szabo, A. G.; Bramall, L.; Krajcarski, D. T. *Rev. Sci. Instrum.* **1985**, *56*, 14.
- (25) James, D. R.; Demmer, D. R. M.; Verrall, R. E.; Steer, R. P. *Rev. Sci. Instrum.* **1983**, *54*, 1121.
- (26) (a) More, J. J. The Levenberg-Marquardt Algorithm: Implementation and Theory. In *Numerical Analysis*, Watson, G. A., Ed.; Springer Verlag: Berlin, 1977; p 105. (b) Garbow, B. S.; Hillstom, K. E.; More, J. J. *Documentation for MINPACK Subroutine LMSTR. Double Precision version*, Argonne National Laboratory, 1980.
- (27) Lakowicz, J. R., Ed. *Topics in Fluorescence Spectroscopy*; Plenum Press: New York, 1991.
- (28) Semenov, A. N., private communication.
- (29) Klushin, L. I.; Skvortsov, A. M. *Macromolecules* **1991**, *24*, 1549.
- (30) For samples I-5 and I-39, PMMA is the minor component, and R_{PI} is recalculated from $R_{PI} = \Phi_{PI}D$, where D is the period spacing. In all the blends examined here, $\Phi_{PI} \leq 0.5$.
- (31) We have some indication from preliminary SAXS experiments (Kuhlmann, T.; Stamm, M., unpublished results) and from transmission electron microscopy measurements (Kressler, J., unpublished results) that at least under some sample preparation conditions both I-39 and I-14 exhibit a cylindrical morphology.
- (32) To match annealing conditions for the SAXS experiments,³¹ a few experiments were carried out after annealing the samples for 2 h at 160 °C or 2 h at 190 °C under vacuum. We had to be very careful to avoid polymer and dye decomposition, and when this was successful, the results obtained were identical to those reported in the text.

MA9612891